Weak bond stretching for three orientations of Ar–HF at $v_{HF}=3$

Cheng-Chi Chuang, Kelly J. Higgins, Henry C. Fu, and William Klemperer

Department of Chemistry and Chemical Biology, Harvard University, 12 Oxford Street, Cambridge, Massachusetts 02138

Three new ArHF ($v_{HF}=3$) states, (3001), (3101), and (3111), have been observed between 11 350 and 11 420 cm^{-1} by the hot band transitions from (0001) using intracavity laser induced fluorescence. The term values and rotational constants of these levels are: (3001) $\nu_0 = 11\,385.928\,98(28)$ cm^{-1}, $B=0.095\,546(32)$ cm^{-1}; (3101) $\nu_0=11\,444.258\,12(68)$ cm^{-1}, $B=0.090\,617(37)$ cm^{-1}; and (3111) $\nu_0=11\,456.076\,51(36)$ cm^{-1}, $B=0.091\,863(14)$ cm^{-1}. Observation of the ArHF (3001) state provides the van der Waals stretching frequency for ArHF at $v=3$, namely 46.8945(4) cm^{-1} = (3001)–(3000). This value shows an increase of 8.208 cm^{-1} (21%) upon HF $v=3\leftarrow 0$ valence excitation. The stretching frequency for the T shaped ArHF is (3111)–(3110) = 33.7055(5) cm^{-1}. This value is only 7% greater than that observed at $v=1$. The ($v_{HF}101$) Σ bend-stretch combination state, corresponding to ($\nu_s=1$) of the Ar–FH configuration, has not been observed at $v_{HF}=0-2$. The stretching frequency here is (3101)–(3100) = 31.8178(8) cm^{-1}. The soft-mode frequencies reveal strong bend-stretch coupling in the complex. Excellent agreement (within 0.3 cm^{-1}) is found between experiment and prediction from Hutson's H6(4, 3, 2) potential [J. Chem. Phys. **99**, 9337 (1993)], for the three new levels. Large basis set coupled cluster calculations [CCSD(T)] of the Ar–HF intermolecular potential surface, $V(R,\theta,r)$, are presented for $r=0.6-2.0$ Å and $\theta=0-180°$ on a grid with 15° spacing. This is an enlargement of the HF valence coordinate of more than double the equilibrium value. The dependence of the intermolecular potential upon the HF valence coordinate, r, is very anisotropic, being maximal for $\theta=0°$ and becoming essentially independent of r for $\theta \geq 45°$. © *2000 American Institute of Physics.* [S0021-9606(00)00516-X]

I. INTRODUCTION

ArHF is by far the most extensively studied weakly bound complex. Presently, a total of 30 vibrational states have been spectroscopically characterized in various wavelength regions, ranging from radiofrequency,[1] microwave,[2] far-infrared,[3] mid-infrared,[4–9] through near-infrared.[10,11] The spectroscopic investigations are a sensitive probe of the Ar–HF interaction potential, not only near the potential minimum but also for angular and increasingly large radial excursions. Of great importance is the accurately determined ArHF ground state ($v=0$) binding energy ($D_0=101.7 \pm 1.2$ cm^{-1}) using absorption spectroscopy of an equilibrium Ar–HF system.[4] On the basis of spectral red-shifts, binding energies of ArHF ($v=1-3$) have subsequently been determined. The recent overtone spectroscopy of ArHF ($v=3$) has made it possible to extend observations of the explicit dependence of the Ar–HF interaction potential on the HF valence coordinate.[10,11] For example, at its outer classical turning point at $v=3$, the HF bond length has increased 35% from its equilibrium value. A further data set is provided by the dissociation dynamics of metastable states of ArHF. Relatively rapid but parity-state dependent rotational predissociation has been observed in the ($vbKn$) = ($v210$)[12] state ($v=1$ and 3).[9,11] Direct measurement of the much slower vibrational predissociation rate, as well as the product state distribution, has been made for two states of ArHF at $v=3$ from dispersed fluorescence.[13] Vibrational predissociation at

$v=2$ is observed[14] to occur in less than 3×10^{-4} seconds for the (2000) level but not for the bending state (2110). These data implicitly contain new detailed potential information which probably cannot be obtained from measurements of bound states.

From a qualitative viewpoint ArHF serves as a model of very weak hydrogen bonding. The levels ($v000$), which have essentially a linear Ar–HF geometry with large amplitude off axis excursion, show a strong enhancement of binding with HF valence excitation, which is typical of hydrogen bonding. The levels ($v110$) have the HF unit essentially perpendicular to the heavy atom axis while the levels ($v100$) have predominantly the linear anti-hydrogen bonded geometry Ar–FH. Both of these configurations, ($v110$) and ($v100$), have shown very little dependence of binding energy upon v_{HF} valence excitation.

In parallel with the experimental studies, there has been a considerable amount of theoretical work in constructing the three-dimensional Ar–HF potential energy surface (PES). High level *ab initio* ArHF PES have been recently reported by Tao,[15] while Dunning[16] has obtained essentially quantitative agreement with Hutson's H6(4,3,2) semiempirical Ar–HF PES[17] at a limited set of critical configurations. The H6(4,3,2) PES is obtained by fitting all existing spectral observables for $v_{HF}=0$, 1, and 2. This is the most complete and accurate presently available PES. Since it has not used $v_{HF}=3$ data, its predictive capabilities may readily be tested. In particular, the dependence of the interaction potential upon

　　　　　7022

J. Chem. Phys., Vol. 112, No. 16, 22 April 2000

Ar–HF at $v_{HF}=3$ 7023

the lower bender state ($j \leq 1$) of ArHF ($v=3$) is well predicted. However, some discrepancies begin to occur at $v=3$ for higher bender states.[11] The H6(4,3,2) Ar–HF pair potential combined with Azis's Ar–Ar pair potential[18] is then used to model the Ar_2HF interaction potential. Hutson and Ernesti[19] have presented a detailed study of this system with estimates of the three-body force. For configurations far from the potential minimum, significant discrepancies between experiment and theory appear to exist. Since three body effects are not large in Ar_2HF, the refinement of the Ar–HF pair potential, particularly its HF valence state dependence, is useful. In this work we report a high level *ab initio* intermolecular potential surface, $V(R, \theta, r)$, which includes $0.6 \leq r \leq 2.0$ Å, and varies θ from 0 to 180° in steps of 15° to provide a detailed picture of the anisotropy of the intermolecular potential and especially the anisotropy of the dependence of the intermolecular potential upon the valence coordinate, r. In $v=3$ the classical turning points of HF are 0.73 and 1.25 Å. It is likely that future work on ArHF will extend measurements to $v=5$, thus it is useful to extend the intermolecular potential surface to include as large extensions of the valence coordinate as is feasible.

Chang *et al.*[10,11] have reported the observation of ArHF (3000), (3110), (3100), (3002), and (3210) overtone transitions via (0000) using intracavity laser induced fluorescence. No success, however, was obtained in the observation of the ArHF (3001)←(0000) transition which would precisely provide the fundamental van der Waals or hydrogen bond stretching frequency for ArHF at $v=3$. From Hutson's H6(4,3,2) potential,[11] the ArHF (3001)←(0000) transition is predicted to be centered at 11 386.2 cm^{-1}, which is embedded in the complex spectrum of the $Ar_2HF(v=3)$ Π in-plane bending band centered at 11 387.7 cm^{-1} (Ref. 20). More than 140 rovibrational transitions, appearing from 11 384 to 11 390 cm^{-1}, were unambiguously assigned to the Ar_2HF $v_{HF}=3 \leftarrow 0$ transition. No prominent, regularly spaced, P and R features in the interval 11 380 to 11 390 cm^{-1} attributable to the ArHF (3001)←(0000) transitions were evident. The transition strength for the above band is thus anomalously weak compared to the fundamental (3000)←(0000) transition, and is not detected with our current sensitivity. The (3001) level can, however, be accessed by the (3001)←(0001) hot band transition, since the (1001)←(0001) transition has been readily recorded by Nesbitt and co-workers.[7] In this paper, we report observation of the ArHF (3001) vdW stretch as well as the (3101) Σ and (3111) Π bend-stretch combination bands obtained from hot band excitation originating from the (0001) state. These states correspond geometrically to Ar–HF (3001), Ar–FH (3101), and T shaped ArHF (3111) and provide the elastic constants for the hydrogen bonded form as well as the nonhydrogen bonded forms.

II. EXPERIMENT

The experimental apparatus has been described in detail previously.[10] Briefly, intracavity laser induced fluorescence has been used to observe the $v_{HF}=3 \leftarrow 0$ valence excitation of the ArHF complex. The ArHF complex, generated in a supersonic slit jet expansion located inside the Ti-sapphire

ring laser cavity, is excited by 40 W of single mode infrared radiation near 900 nm. The ArHF hot band signal is optimized when the corresponding ArHF (3000)←(0000) signal is maximized. The best stagnation condition for forming the ArHF complex is ~1% HF seeded in Ar at 700 Torr. The excitation is $\Delta v_{HF}=3$, and overtone emission ($\Delta v_{HF}=-2$) is collected by a liquid N_2 cooled germanium detector. Because of the long radiative lifetimes and the high translational velocity of the complexes in the jet, less than 1% of the total fluorescence is emitted during the observation time, corresponding to the flight distance of 7 mm.

Amplitude modulation (AM) is used for the signal detection scheme. The Ar ion laser is currently 90% amplitude modulated by an acousto-optic modulator. The Ti-sapphire laser is frequency stabilized to the power maximum of the cavity mode, which produces an observed frequency stability somewhat better than 10 MHz. With the current AM detection scheme and significant reduction of the scattered laser radiation reaching the detector, the signal-to-noise (S/N) has been improved by a factor of 3 compared to previous reports from this laboratory. This allows us to readily record the associated ArHF ($v=3$) hot band transitions originating from ArHF (0001).

Because of the lack of reference gas standards in this wavelength region, accuracy of the absolute frequency presently depends on a homemade wavemeter and a calibrated Fabry–Perot interferometer. Frequencies of the rovibrational lines of the complex are determined as follows. The absolute laser frequencies are measured before and after the scanning of every 20 GHz spectral range. Positions of the observed lines are then determined by linear interpolation within the 1.45 GHz etalon frequency marks. Standard deviation of the absolute frequency uncertainty is less than ± 0.003 cm^{-1}. The relative frequency is considerably more accurate.

III. RESULTS AND ANALYSIS

The assumption of thermal equilibrium between rotation and the intermolecular vibrations gives a 15 K vibrational temperature for the jet. The (3001)←(0001) hot band transition intensity is reduced by a Boltzmann factor of approximately 0.02 compared to that of (3000)←(0000) [the (0001) state is situated 38.6863 cm^{-1} above the (0000) state[7]]. The S/N for the (3000)←(0000) transition is presently 3000/1 (time constant=1 s); thus the corresponding vdW stretch hot band transition with S/N=60 should be readily observable. Similarly, the stretch-bend combination hot band transitions (3111)←(0001) and (3101)←(0001), correlated with Ar+HF($v=3,j=1$), should also be observed without difficulty. The search for these three bands was very effectively guided by the existing predictions from Hutson's H6(4,3,2) potential.[11] The analysis of the observed transitions is readily accomplished since the term values for the lower level (0001) are well established by Nesbitt and co-workers.[7]

A. The ArHF (3001)←(0001) band

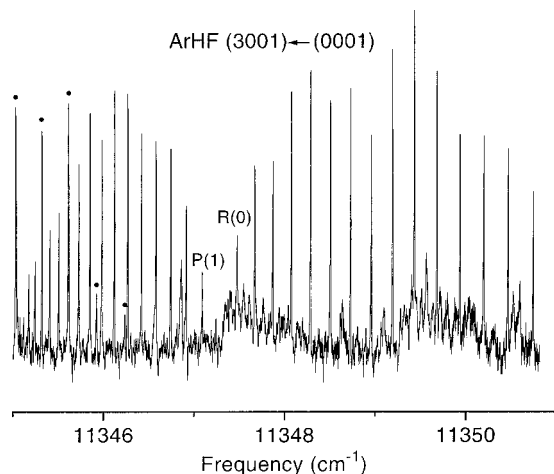About 7 cm^{-1} to the blue of the ArHF (3000)←(0000) band we have observed a spectrum with P and R branches,

FIG. 1. Action spectrum of the ArHF $(3001) \leftarrow (0001)$ hot band transitions centered at 11 347.2 cm^{-1}. The spectrum was recorded with a single scan with intracavity power of 40 W and a time constant of 3 s. The band origin yields the ArHF ($v=3$) vdW stretch frequency to be 46.894 cm^{-1}. Features labeled by ● are R branch lines of the ArHF $(3000) \leftarrow (0000)$ band centered at 11 339.0 cm^{-1} (Ref. 10).

TABLE II. Spectroscopic constants (in cm^{-1}) of the ArHF (3001), (3101), and (3111) states.

	Expt.	$H6(4,3,2)$ calc.[a]
$\nu_0(3001)$	11 385.928 98(28)	11 386.106
$\nu_0(3001) - \nu_0(3000)$	46.8945(4)	47.150
$B(3001)$	0.095 546(32)	0.095 61
$D_J(3001) \times 10^{-6}$	2.65(26)	
$\nu_0(3101)$	11 444.258 12(68)	11 444.481
$\nu_0(3101) - \nu_0(3000)$	105.2237(7)	105.525
$B(3101)$	0.090 617(37)	0.090 05
$D_J(3101) \times 10^{-6}$	2.696(38)	
$\beta_{\langle 3101|3111\rangle}$	0.155 86(15)	
$\nu_0(3111)$	11 456.076 51(36)	11 456.173
$\nu_0(3111) - \nu_0(3000)$	117.0420(4)	117.217
$B(3111)$	0.091 863(14)	0.090 47
$D_J(3111) \times 10^{-6}$	4.91 (12)	
$q_l(3111)$	0.002 085(19)	
$q_d(3111) \times 10^{-7}$	8.5(2.0)	

[a]The calculated values are taken from Ref. 11.

centered at 11 347.2 cm^{-1} (predicted band center 11 347.4 cm^{-1}), as shown in Fig. 1. The spectrum can be characterized as $\Sigma \leftarrow \Sigma$ type rovibrational transition of a linear molecule. As expected, the integrated band intensity is approximately 60 times weaker than that of the corresponding $(3000) \leftarrow (0000)$ band. The S/N allows the observation of lines with J up to 16. The decrease (increase) in the rotational line spacing in the P-branch (R-branch) as J increases indicates a significant increase in the B rotational constant upon HF valence excitation. The measured linewidth, 140 MHz, is identical to that of ArHF (3000) and its combination bands reported previously, and is consistent with a pure Doppler profile at 15 K. Lower state combination differences

establish that this band originates from ArHF (0001). This band is unambiguously assigned to the hot band transition of ArHF $(3001) \leftarrow (0001)$.

The observed rovibrational transitions are fitted with the standard polynominal expansion in $J(J+1)$ for a semi-rigid linear molecule for both vibrational levels

$$E_v(J) = \nu_0(v) + B(v)[J(J+1)] - D(v)[J(J+1)]^2. \quad (1)$$

By fixing the lower (0001) state term values to those determined from Lovejoy *et al.*,[7] the spectrosopic constants of (3001) can be readily obtained. The observed (and calculated) term values and fitted spectroscopic constants for the (3001) state are listed in Tables I and II, respectively. The

TABLE I. Observed and calculated term values (in cm^{-1}) of the (0001), (3001), (3101), and (3111) states of ArHF.[a]

	$E_v(J) - \nu_0(0000)$				
J	(0001)[b]	(3001)	(3101)	(311^e1)	(311^f1)
0	38.6863	11 385.8334(3)			
1	38.8714	11 386.0245(−3)		11 456.1705(6)	
2	39.2414	11 386.4066(−1)	11 444.7111(2)	11 456.5419(7)	11 456.5294(4)
3	39.7962	11 386.9797(3)	11 445.2546(−1)	11 457.0989(3)	11 457.0738(3)
4	40.5355	11 387.7434(4)	11 445.9789(−1)	11457.8408(1)	11457.7991(3)
5	41.4590	11 388.6976(−7)	11 446.8837(0)	11 458.7673(9)	11 458.7047(−18)
6	42.5662	11 389.8419(−1)	11 447.9689(−4)	11 459.8776(13)	11 459.7900(−11)
7	43.8565	11 391.1759(0)	11 449.2339(4)	11 461.1709(−7)	11 461.0542(−1)
8	45.3294	11 392.6992(−3)	11 450.6783(−5)	11 462.6464(1)	11 462.4963(3)
9	46.9840	11 394.4113(0)	11 452.3017(−3)	11 464.3029(−1)	11 464.1152(11)
10	48.8195	11 396.3114(3)		11 466.1390(6)	11 465.9097(−6)
11	50.8349	11 398.3990(−2)		11 468.1535(2)	11 467.8783(−6)
12	53.0292	11 400.6732(−1)		11 470.3446(−4)	11 470.0194(12)
13	55.4011	11 403.1333(−6)			11 472.3311(7)
14	57.9493	11 405.7781(−1)			11 474.8115(1)
15	60.6723	11 408.6068(−5)			11 477.4584(−19)
16	63.5685	11 411.6182(8)			11 480.2692(9)

[a]The standard deviation in frequency measurements is ±0.0007 cm^{-1}. Numbers in parentheses are deviations (observed minus calculated) in units of the last significant digits.
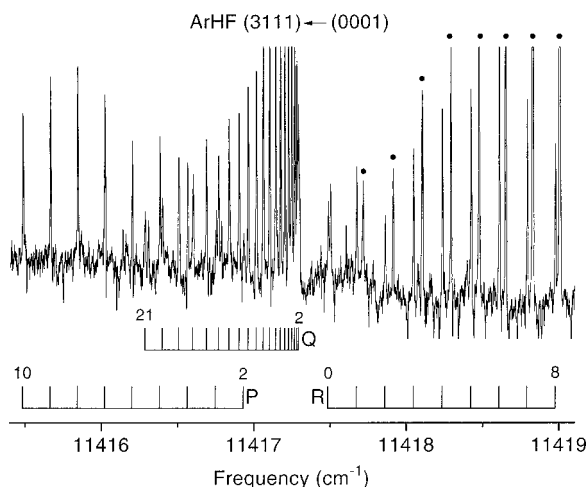[b]Calculated from Ref. 7.

J. Chem. Phys., Vol. 112, No. 16, 22 April 2000

Ar–HF at $v_{HF}=3$ 7025

FIG. 2. Action spectrum of the ArHF $(3111)\leftarrow(0001)$ hot band transition centered at 11 417.4 cm^{-1}. The spectrum was recorded under the same experimental conditions as Fig. 1. Features labeled by ● are P branch lines of the ArHF $(3110)\leftarrow(0000)$ band centered at 11 422.3 cm^{-1} (Ref. 10).

FIG. 3. Action spectrum of the ArHF $(3101)\leftarrow(0001)$ hot band transition centered at 11 405.5 cm^{-1}. The spectrum was recorded under the same experimental conditions as Fig. 1. This band is overlapped with much broader linewidth features (Lorentzian linewidth of 2.5 GHz), labeled by ●, which are attributed to the R branch of the $K=0\leftarrow0$ subband of the $3v_1+v_4$ mode of (HF)$_2$ centered at 11 402.8 cm^{-1} (Ref. 21).

$(3001)\leftarrow(0001)$ band origin (ν_0) and (3001) state rotational constant, B, obtained from the fit are 11 347.2426(3) cm^{-1} and 0.095 546(32) cm^{-1}, respectively. The (3001) band is 46.894 cm^{-1} above the (3000) band and the heavy atom stretching frequency at $v=3$ is thus accurately determined. The rotational constant is 90 MHz larger than that of the (0001) state, $B=0.092\,543\,4$ cm^{-1}. The vdW stretch frequency increases 8.208 cm^{-1} (21%) upon HF $v=3\leftarrow0$ valence excitation compared to that of 2.64 cm^{-1} (6.8%) upon HF $v=1\leftarrow0$ excitation.[7] The B rotational constant shows significant reduction, 229 MHz (7.4%), compared to that of (3000), which indicates a 0.13 Å average elongation of the vdW bond length upon its stretching excitation. The centrifugal distortion constant D, however, decreases from the value observed for the (0001) state. The change in both the B and D constants is consistent with those observations at $v_{HF}=1-3$ that the intermolecular bond is strengthening upon HF valence excitation.

B. The ArHF $(3111)\leftarrow(0001)\Pi$ bend

Similar to the previous observation of the ArHF (3100) and (3110) bending states, which asymptotically correlate to HF $j=1$ $v=3$, we have presently observed ArHF (3111) and (3101) bend-stretch combination bands originating from the lower (0001) state. Figure 2 shows the spectrum with P, Q, and R branches centered at 11 417.4 cm^{-1} (predicted center $=11\,417.4$ cm^{-1}) and can be characterized as a $\Pi\leftarrow\Sigma$ type transition. The integrated band intensity is about 2.5 times weaker than that of the preceding ArHF $(3001)\leftarrow(0001)$ band. We then assign this band to the hot band transitions of ArHF $(3111)\leftarrow(0001)$.

C. The ArHF $(3101)\leftarrow(0001)\Sigma$ bend

The ArHF (3100) Σ bend is predicted ~10 cm^{-1} below the (3110) Π bend. About 12 cm^{-1} to the red of the $(3111)\leftarrow(0001)$ transition we have observed some sharp lines embedded within the previously reported (HF)$_2$ $3v_1$
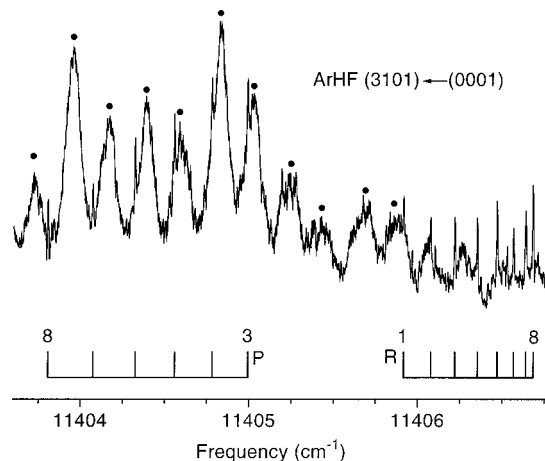
$+v_4$ ($K=0$) subband centered at 11 402.8 cm^{-1} (see Fig. 2 in Ref. 21), as shown in Fig. 3. The (HF)$_2$ features are distinguished by their broad linewidths (3 GHz). The sharp features, consisting of a P and an R branch, indicate a $\Sigma\leftarrow\Sigma$ type transition. The S/N of the strong R lines is about half that of the corresponding $(3111)\leftarrow(0001)$ transition. Lower state combination differences confirm these transitions originate from ArHF (0001). The band center is about 0.3 cm^{-1} lower than that predicted by Hutson's H6(4, 3, 2) potential. We assign this band to the ArHF $(3101)\leftarrow(0001)$ Σ bend.

D. Analysis of the (3111) and (3101) levels

In Table I we list the term values of the (311^f1), (311^e1), and (3101) states. These are constructed by adding the term values of (0001) to the observed $(3111)\leftarrow(0001)$ Q branch lines, the observed $(3111)\leftarrow(0001)$ P/R branch and the observed $(3101)\leftarrow(0001)$ lines, respectively. To obtain the spectroscopic constants of the (3111) and (3101) states, the fitting consists of two parts. First, we simply fit the observed e and f parity levels of the (3111) state by the standard Hamiltonian of a linear molecule with nonzero vibrational angular momentum l:

$$E_v(J)_{e/f}=\nu_0(v)+B(v)[J(J+1)-l^2]$$
$$-D(v)[J(J+1)-l^2]^2$$
$$\pm1/2\{q_lJ(J+1)-q_d[J(J+1)]^2\}. \quad (2)$$

This fitting procedure provides the standard spectroscopic constants for the l-type doubling (3111) level. The spectroscopic constants of the (3111) state obtained from the fit are listed in Table II. The standard deviation of the fit is 0.0009 cm^{-1}, slightly larger than the experimental uncertainty of 0.0007 cm^{-1}. The l-doubling constant of the (3111) state is 0.002 08(2) cm^{-1} (62.4 MHz). Note that the positive sign of the l-doubling constant is consistent with the observation that the (311^e1) level is positioned above (311^f1).[22] A somewhat more physical view is afforded by treating the Coriolis

interacting (311^e1) and (3101) levels to obtain their unperturbed spectroscopic constants. We have performed the standard deperturbation analysis, analogous to the previous analysis for ArHF $v=1$ (Ref. 7) and $v=3$ (Ref. 10) states with no vdW stretch, $(v100)$ and $(v11^e0)$. We deperturb the strongly Coriolis interacting (3101) and (311^e1) bends by simultaneously least-squares fitting the observed P/R branch levels (with e parity) in both states to a 2×2 Hamiltonian matrix

$$\hat{\mathbf{H}} = \begin{vmatrix} H_{11} & H_{12} \\ H_{21} & H_{22} \end{vmatrix} \tag{3a}$$

with matrix elements defined by

$$H_{11} = \nu_0(3111) + B(311^e1)[J(J+1) - l^2]$$
$$\quad - D(311^e1)[J(J+1) - l^2]^2,$$

$$H_{22} = \nu_0(3101) + B(3101)[J(J+1)]$$
$$\quad - D(3101)[J(J+1)]^2, \tag{3b}$$

$$H_{12} = H_{21} = \beta[J(J+1)]^{1/2}.$$

The off-diagonal matrix element represents the phenomenological Coriolis coupling term connecting two states with $|l| = 1(\Pi)$ and $0(\Sigma)$, which we discuss further below. The constants of $\nu_0(311^e1)$, $B(311^e1)$ and $D(311^e1)$, as above are the unperturbed values. These must be the same as those determined by fitting the unperturbed (311^f1) levels. Since the displacement of the (3101) levels is equal and opposite to that of the (311^e1) levels in this model, the position of the unperturbed values $H_{22}(J)$ are determined by subtracting the observed e-f displacement of the (3111) levels from the observed term values of (3101). The value of $\beta^2[J(J+1)]$ is readily obtained by linearization of Eq. (3a), since the highest relevant e-f displacement of the (3111) levels, at $J=9$, is less than 2% of the (3111)–(3110) separation. The deperturbed spectroscopic constants obtained from this analysis are listed in Table II. The standard deviation of the fit is 0.0009 cm^{-1}, which is very close to the experimental error of 0.0007 cm^{-1}. This justifies the present two-state deperturbation of the interaction of the (3101) Σ bend with the $(311^e1)\Pi^e$ bend. The nearby vdW stretching states of (3003) [predicted 9 cm^{-1} below] and (3004) [predicted 6 cm^{-1} above] impose negligible perturbation on the (3101) Σ bend state. This is in sharp contrast to the previous study of ArHF $(v100)$ and $(v11^e0)$ [$v=0-3$], where the $(v002)$ vdW stretching state is in resonance with the $(v110)$ state [$v=0-3$] and the deperturbation requires taking interaction with the $(v002)$ state into account. In the present case there are no such close resonances: thus it is sufficient to treat the interaction between the related levels arising from $j=1$, $v=3$HF with one quantum of van der Waals stretch.

The deperturbed (3101) and (3111) vdW bend-stretch levels are 105.2237 cm^{-1} and 117.0420 cm^{-1} with respect to the (3000) state, respectively. The energy splitting between these two states is 11.8183 cm^{-1}. The corresponding energy splitting between (3100) and (3110) bending states is 9.935 cm^{-1}, which is 1.883 cm^{-1} smaller than that between (3101)

and (3111). We return to this apparently surprising result in the discussion section following the presentation of our *ab initio* calculations.

IV. *AB INITIO* CALCULATIONS

The complete discussion of the *ab initio* calculations will be presented elsewhere.[23] In brief, the three-dimensional intermolecular potential surface of Ar–HF, $V(R,\theta,r)$, is calculated using the CCSD(T) method with a basis consisting of Dunning and co-workers' aug-cc-pVTZ basis set[24–26] supplemented with $[3s3p2d]$ bond functions.[27] It is necessary to use the CCSD(T) method rather than the less expensive MP4 method in order to properly describe the HF molecule at long HF bond distances. Although the MP4 method does a slightly better job of calculating the potential energy curve for HF, recovering 99% of the well depth versus 98% for CCSD(T) when compared to an experimentally determined potential,[28] it does a very poor job of calculating the dipole moment function at long HF bond distances. When compared to an *ab initio* dipole moment function that is in excellent agreement with experiment,[29] the MP4 dipole moment function begins to diverge significantly at an HF bond distance of 1.5 Å and by 2.0 Å it is 33% too large. In contrast, the CCSD(T) dipole moment function stays within 1% between 0.6 and 1.7 Å, and at 2.0 Å it is just 5.5% too large. The basis has been used with other argon-molecule complexes in the past with success,[30] and when compared to the benchmark calculations of van Mourik and Dunning[16] gives binding energies for Ar–HF within 0.5% of their largest atom centered basis and within 2.4% of the estimated complete basis set limit for each of the three main configurations.

Interaction energies are calculated using the supermolecular approach with the complete Boys–Bernardi[31] counterpoise correction on a grid of 16 radial points with 2.5 $\leq R \leq 10.0$ Å, 13 angular points with $0 \leq \theta \leq 180°$ in increments of 15°, and 19 HF bond distances with $0.6 \leq r \leq 2.0$ Å, for a total of 3458 geometries. All *ab initio* calculations are performed using the MOLPRO 98.1 package,[32] and interpolation between grid points is performed using a three-dimensional cubic spline routine.[33]

Previous *ab initio* and empirical intermolecular potentials for ArHF[11,15–17,34] have concentrated on HF bond distances near equilibrium or for lower vibrational states using the vibrationally averaged bond distance for the state. Only limited averaging of the potential over the vibrational state has been performed and no calculations reaching to the inner or outer classical turning points of HF for $v=3-5$ have been presented. Even at the classical turning points there is substantial probability density, making it necessary to calculate the intermolecular potential for long HF bond distances in order to fully understand the bound state and vibrational predissociation dynamics of ArHF at HF $v=3-5$.

Results of the *ab initio* calculations are presented graphically in Figs. 4–6. The global minimum in the intermolecular potential (ignoring the HF potential) is -521.0 cm^{-1} and occurs at $R=3.45$ Å, $\theta=0°$, with an HF bond distance of 1.50 Å, over 60% longer than the equilibrium HF bond length of 0.9168 Å. The effect of stretching the HF bond on the intermolecular potential, shown in Fig. 4(a), is highly

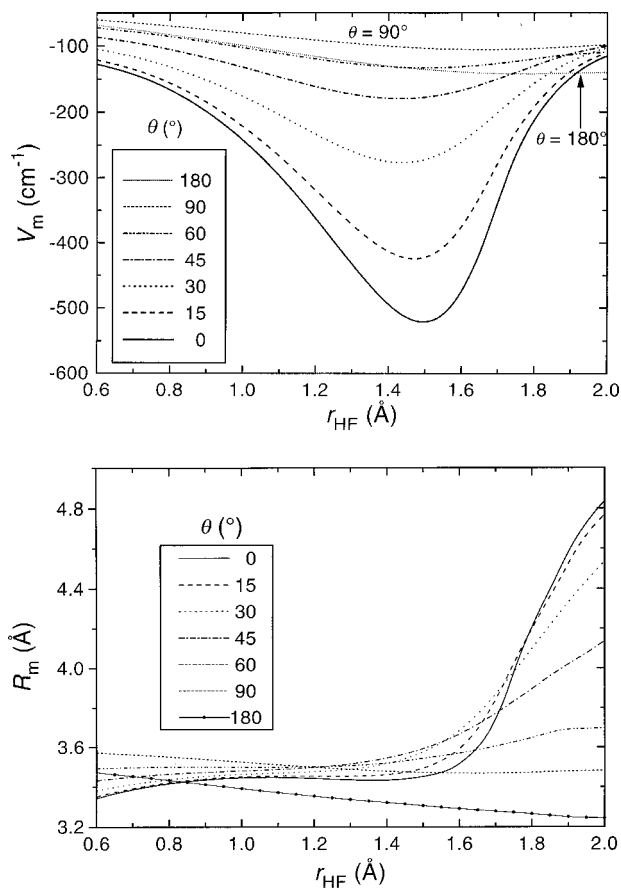J. Chem. Phys., Vol. 112, No. 16, 22 April 2000

Ar–HF at $v_{HF}=3$ 7027

FIG. 4. Minimum energy path for the CCSD(T) potential surface of Ar–HF as a function of HF bond distance. (a) Cuts along constant θ of the minimum potential energy. By $\theta=45°$ the dependence on the HF bond distance has virtually disappeared. (b) The radial distance, R, at which the minimum energy in (a) occurs. This remains essentially constant from $r=0.6$ to 1.5 Å for all values of θ. Beyond $r=1.5$ Å values of $\theta \leqslant 45°$ show a sharp increase in radial distance as the repulsion between the argon and the hydrogen begins to be felt.

FIG. 5. (a) Minimum energy path for the CCSD(T) potential surface of Ar–HF as a function of θ. The HF bond distances shown correspond to the HF $v=4$ classical inner and outer turning points (0.716 and 1.318 Å), the HF $v=0$, 3, and 4 vibrationally averaged distances (0.932, 1.032, and 1.063 Å), and the position of the global minimum on the Ar–HF interaction energy surface (1.500 Å). The anisotropy increases dramatically upon stretching the HF bond. As seen in Fig. 4, almost all of the change comes at $\theta \leqslant 45°$. (b) Cuts at constant R on the two-dimensional potential corresponding to $v_{HF}=3$. Values of R shown, 3.54, 3.74, and 4.04 Å, correspond to $\langle R \rangle$ from collocation calculations for ArHF states (3000), (3001), and (3002) respectively.

anisotropic, with the greatest effect occurring at $\theta=0°$ and with almost no effect for $\theta \geqslant 45°$. For all angular configurations the value of R at the minimum energy position, presented in Fig. 4(b), remains quite constant upon stretching the HF bond distance through the equilibrium region and out to $r=1.5$ Å. Beyond $r=1.5$ Å the effects of repulsion between the hydrogen and the argon are seen in the lower angles as the value of R at the minimum energy position begins to increase dramatically. The anisotropy of the potential for several fixed values of the HF bond distance is shown in Fig. 5. This also shows the dramatic increase in anisotropy upon stretching of the HF bond.

In order to assess the quality of the *ab initio* potential it is necessary to calculate the bound states for the potential and to compare them with the experimentally determined bound states. Full three-dimensional quantum calculations of the bound states are beyond the scope of the present paper and will be presented elsewhere.[23] Instead, two-dimensional potential surfaces for the interaction of HF in a particular vibrational state with argon have been generated by averaging the full three-dimensional potential over the HF vibrational state of interest:
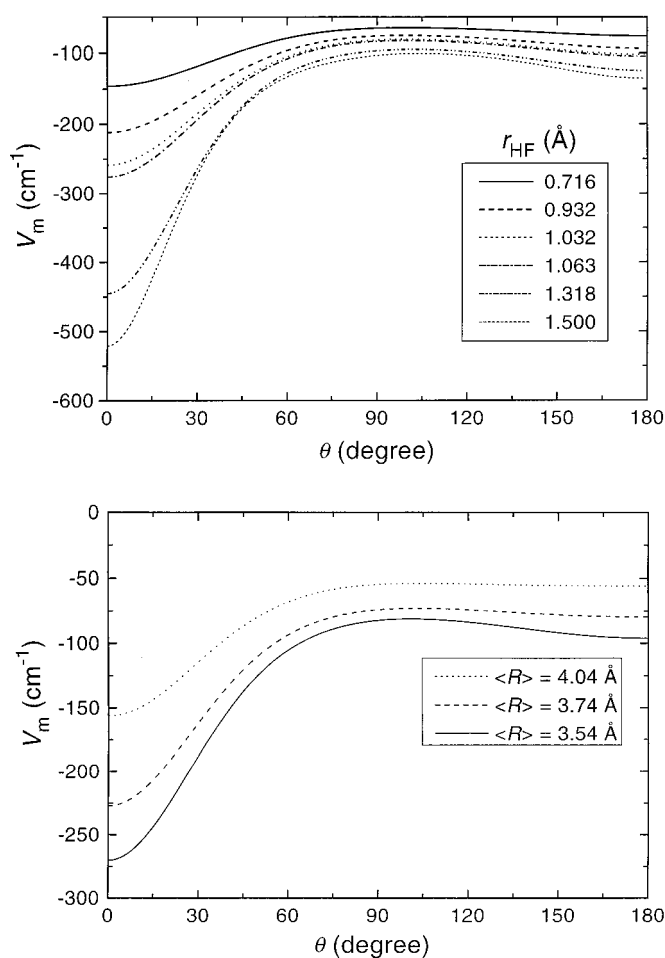
$$\bar{V}(R,\theta) = \langle \nu(r) | V(R,\theta,r) | \nu(r) \rangle, \qquad (4)$$

where $\nu(r)$ is the vibrational wave function for HF generated by a variational calculation on an empirical HF potential energy curve.[29] Averaging the potential over the $v=3$ HF vibrational state deepens the potential by 6.6% in the linear Ar–HF configuration while lessening the potential by 0.4% for the anti-linear Ar–FH configuration and 0.2% for the T shaped configuration when compared to *ab initio* calculations using an HF distance fixed at its $v=3$ vibrationally averaged distance of 1.0324 Å. Comparing the potential averaged over $v_{HF}=3$ to Hutson's H6(4,3,2) potential shows that the present potential recovers 98.3% of the H6(4,3,2) well depth at $\theta=0°$, 94.5% at $\theta=90°$, and 98.8% at $\theta=180°$, while overestimating R_m by 0.038, 0.025, and 0.007 Å for the three configurations, respectively.

Bound states for the two-dimensional potential surfaces are calculated using two different programs: a modified ver-
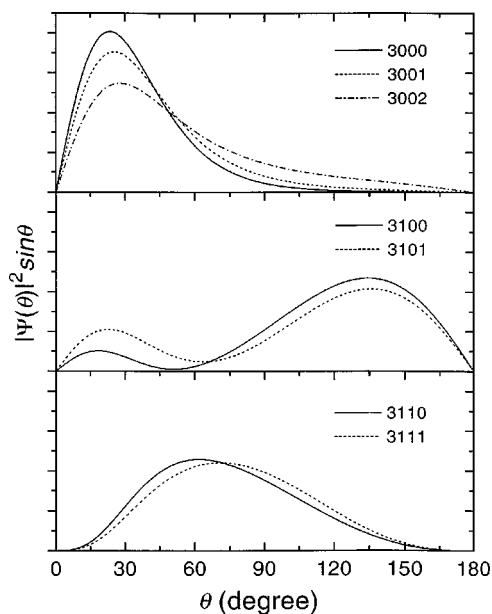
FIG. 6. The effect of van der Waals stretching on the angular distribution functions of three ArHF ($v_{HF}=3$) bending states. Calculated by integrating the two-dimensional global distribution function, $|\Psi(R,\theta)|^2 R^2 \sin\theta$, over R. The wave functions are produced from a collocation calculation on the two-dimensional potential corresponding to $v_{HF}=3$, and the distribution functions vanish at 0 and 180° due to the $\sin\theta$ term in the volume element.

sion of the collocation program from Cohen and Saykally,[35] and the BOUND program of Hutson.[36] Well-converged bound state energies are calculated using BOUND, while the collocation method produces bound state wave functions that BOUND does not. Agreement to better than 0.003 cm^{-1} between the two programs for the bound state energies provides a check of the consistency of the computational methods. Results of the bound state calculations for the HF $v=3$ states in terms of binding energies are presented in Table III. Agreement between theory and experiment is reasonable and is expected to be better with full three-dimensional calculations as will be discussed later. The angular distribution functions of these states are presented graphically in Fig. 6. These distribution functions are generated from the wave functions calculated using the collocation method by integrating the two-dimensional global distribution function, $|\Psi(R,\theta)|^2 R^2 \sin\theta$, over R.

TABLE III. Binding energies (in cm^{-1}, relative to HF $v=3$, $J=0$) of HF $v=3$ states of ArHF from experiment and theory.

$(vbKn)$	*ab initio* calculation	Experiment[a]
(3000)	−123.098	−135.473
(3001)	−78.624	−88.578
(3100)	−56.506	−62.067
(3002)	−45.083	−52.361
(3110)	−45.136	−52.132
(3101)	−25.277	−30.249
(3111)	−13.187	−18.431
(3210)	9.754	10.238

[a]Derived from the binding energy of (0000) from Ref. 4, and data reported in Ref. 11 and in this work. Although the absolute binding energies are limited by the ±1.2 cm^{-1} uncertainty in D_0 for (0000), the relative binding energies are good to ±0.004 cm^{-1}.

V. DISCUSSION

The fundamental van der Waals (or hydrogen bond stretching) frequency, 46.894 cm^{-1}, of ArHF at $v=3$ is obtained by the observation of the ArHF $(3001)\leftarrow(0001)$ hot band transition. In conjunction with the previous precision measurements of ArHF [38.686 cm^{-1} at $v=0$ (Ref. 3) and 41.334 cm^{-1} at $v=1$ (Ref. 7)], the vdW stretch frequency increases linearly upon HF valence excitation, being fitted as

$$\omega(v00)=(v001)-(v000)$$
$$=38.649(1+0.070\,95v)\ \text{cm}^{-1}. \quad (5)$$

The corresponding frequency for ArHF at $v=2$ has not been reported yet, but is estimated by Huston[17] to be 44.202 cm^{-1}. Use of Eq. (4) gives a vdW stretch frequency of 44.133 cm^{-1} for ArHF at $v=2$, showing nearly perfect agreement with the prediction. We emphasize a significant enhancement of 8.208 cm^{-1} (21.2%) in the stretching frequency for the linear hydrogen bonded form upon HF $v=3\leftarrow0$ valence excitation. Together with the previously observed (3002) state, 83.112 cm^{-1} above (3000), the observation of ArHF ($v=3$) heavy atom stretching states ($\nu_s=0-2$) provides a sensitive probe for the radial part of the Ar–HF ($v=3$) potential. The considerable anharmonicity in the radial potential is evident by the reduction in the $(3002)\leftarrow(3001)$ stretch frequency to 36.218 cm^{-1} compared to 46.894 cm^{-1} for $(3001)\leftarrow(0000)$. The data may be fitted by an anharmonic oscillator with $\omega_e=57.57$ cm^{-1} and $\omega_e x_e=5.338$ cm^{-1}. Furthermore, the naive approximation based on the harmonic model estimates the (3001) vdW stretch frequency, given by $[4B(3000)^3/D(3000)]^{1/2}$ (Ref. 37), to be 51.9 cm^{-1}, which lies midway between the $\omega_e=57.57$ cm^{-1} and (3001) $\leftarrow(3000)=46.894$ cm^{-1}. According to the calculation based on Hutson's H6(4,3,2) potential, there are in total six ($\nu_s=0-5$) vdW stretching states supported in the Ar–HF ($v=3,j=0$) well ($D_0=135.107$ cm^{-1}). We may note that a simple linear Birge–Sponer extrapolation predicts $D_0=\omega_e^2/4\omega_e x_e=155.2$ cm^{-1}. This is essentially equivalent to treating the (300n) states as a diatomic Morse oscillator. Since the angular anisotropy is largest near the linear hydrogen bonded Ar–HF configuration, it would seem likely that the (300n) states are the poorest for a diatomic representation of the radial dependence of the energy.

The stretching vibrational frequencies of the three Ar–HF orientations are taken to be $\omega(3bK)=(3bK1)-(3bK0)$. These are readily obtained from Table I to be $\omega(300)=46.8945$ cm^{-1}, $\omega(311)=33.7055$ cm^{-1}, and $\omega(310)=31.8178$ cm^{-1}. These may qualitatively be regarded as the structures linear Ar–HF, T shaped Ar–HF and linear Ar–FH. The valence vibrational dependence of the latter terms cannot be determined from existing experimental observations. It is, however, possible to use the accurate calculations of Hutson for this purpose. These give $\omega(011)=(0111)-(0110)=30.561$ cm^{-1} and $\omega(010)=(0101)-(0100)=32.173$ cm^{-1}. While at $v_{HF}=1$ (Ref. 7), $\omega(111)=(1111)-(1110)=31.480$ cm^{-1} and $\omega(110)=(1101)-(1100)=32.452$ cm^{-1}. It is clear that the valence vibration dependence of the stretching frequencies of the three configurations is strongest for the linear Ar–HF arrangement.

The valence vibrational dependence of the stretching frequency of the $j=1\ \Sigma$ state, $\omega(v10)$, is surprising. The values show a parabolic behavior. We note that the values of $\omega(010)$ and $\omega(110)$ are those calculated by Hutson.[17] At first sight it would be tempting to ascribe the nonlinear dependence as an artifact of the calculation, however, the calculated value of $\omega(310)=32.018\ \text{cm}^{-1}$ is in good agreement with the measurement of $31.8178\ \text{cm}^{-1}$.

While the binding energies calculated using the *ab initio* potential are off by up to $12.4\ \text{cm}^{-1}$ in an absolute sense, the relative energies are well predicted. The *ab initio* potential predicts for the stretching frequencies: $\omega(300)=44.474\ \text{cm}^{-1}$, $\omega(311)=31.949\ \text{cm}^{-1}$, and $\omega(310)=31.229\ \text{cm}^{-1}$. In addition, the $\Sigma-\Pi$ splitting is well represented by the *ab initio* calculations, giving a splitting in the $(3bK0)$ states of $11.370\ \text{cm}^{-1}$ and in the $(3bK1)$ states of $12.090\ \text{cm}^{-1}$. The largest discrepancies come when comparing the $j=1\ \Sigma$ and Π energy levels, $(310n)$ and $(311n)$, with (3000). This is most likely the result of ignoring the dynamic effects the presence of the argon will have on the HF vibrational wave function and energy. The linear Ar–HF arrangement of (3000) should be expected to have a much greater effect on the HF vibration than the T shaped $(311n)$ or anti-linear Ar–FH $(310n)$ arrangements. Full three-dimensional bound state calculations will be necessary to elucidate this effect.

The linear increase in the intermolecular vdW stretching frequency of ArHF upon HF valence excitation $(v_{HF}=0-3)^{3,7,8,10}$ reflects the nature of the intermolecular bonding between Ar and HF. The Ar–HF $(v=3)$ binding energy, D_0, is increased by $\sim 30\%$ when the average HF valence bond is elongated from $r_{HF}=0.93\ \text{Å}$ $(v_{HF}=0)$ to $r_{HF}=1.03\ \text{Å}$ $(v_{HF}=3)$, as is evident by the increase in spectral red-shift of $33.3\ \text{cm}^{-1}$.[10] The strengthening of the Ar–HF $(v=3)$ bond accordingly accounts for the increase in the vdW stretching frequency upon HF (3-0) valence excitation. The force constant for bond stretching increases rapidly, being almost twice as large at $v=3$ than at $v=0$.[3] We may note that this rapid increase in binding energy and bond stretching force constant is highly directional. The energetics of the three forms $(v000)$, $(v110)$, and $(v100)$, as measured from their asymptotic HF rotational level, are

$$(v000)=101.70[1+0.087\,04v+0.007\,88v^2]\ \text{cm}^{-1},$$

$$(v110)=77.006[1+0.041\,84v+0.003\,14v^2]\ \text{cm}^{-1}, \qquad (6)$$

$$(v100)=90.755[1+0.032\,20v-0.001\,01v^2]\ \text{cm}^{-1}.$$

While the linear Ar–HF, $(v000)$, energy increases rapidly with v, the valence vibrational dependence observed is similar to the vibrational dependence observed for the bond stretching frequency $\omega(v00)$, rather than for the effective force constant, which scales as $\omega^2(v00)$, as might have been expected. The parabolic behavior observed for the Ar–FH configuration $\omega(v10)$, is not seen in the energy $(v100)$. These observations together with the fact that Hutson's H6(4,3,2) potential fits quantitatively all of these features argues strongly against the fitting of a series in which large amplitude angular motions occur with an effective radial potential.

Our *ab initio* calculation results have shown that the r_{HF} dependence of the Ar–HF interaction potential is extremely anisotropic, in that the significant increase in the well-depth for linear Ar–HF is indeed observed, but not for the T shaped or anti-linear geometries, as r_{HF} is varied from 0.6 to 1.5 Å. We may note that the Hartree–Fock energy is essentially independent of HF bond length and somewhat repulsive in the linear configuration showing that the charge distributions of hydrogen fluoride and argon are overlapping and that the effects of electron exchange cannot be ignored, since they are slightly larger than the electrostatic inductive effects. Since as been shown there is good agreement between *ab initio* results and Hutson's H6(4, 3, 2) potential or equivalently experiment, the Ar–HF interaction and its valence coordinate dependence are determined in large measure by the highly anisotropic effects of electron correlation or dispersion forces.

The rotational constants of the different bending states of ArHF show a very slight dependence upon HF valence vibration. For the three soft mode bending states the rotational constants may be summarized as:

$$B(v000)=0.102\,258(1+0.003\,788v+0.000\,13v^2)\ \text{cm}^{-1},$$

$$B(v110)=0.100\,006(1-0.000\,570v+0.001\,48v^2)\ \text{cm}^{-1}, \qquad (7)$$

$$B(v100)=0.102\,226(1+0.003\,837v-0.001\,02v^2)\ \text{cm}^{-1}.$$

This shows first that the orientation of the HF unit has an almost negligible effect upon the heavy atom separation. Second, this independence is essentially independent of the HF valence vibrational state, v. The details of Fig. 4(b) show that this behavior is fully predicted by the *ab initio* calculations. It is noteworthy that the strong dependence of the intermolecular interaction energy upon orientation and HF valence vibrational state is not reflected in the heavy atom separation. The levels $(v000)$ which are closest to the colinear Ar–HF geometry show the strongest energy dependence upon HF valence vibrational state, and might be expected to exhibit an increase in heavy atom separation with stretching of the HF valence coordinate. That this does not, however, occur is seen from the above $B(v000)$. For example, the classical outer turning point of HF at $v=3$ is 0.4 Å greater than r_e, and if a harsh hard sphere repulsion existed we would expect $B(v000)$ to show a dramatic decrease with v rather than the mild increase observed. The expectation of an increase in heavy atom separation with stretching of the HF valence coordinate is essentially based on a very old and certainly incorrect view of rigid atom–atom interactions. The results represented in Figs. 4, 5, and 6 show clearly that this picture is incorrect for Ar–HF interactions and probably for all hydrogen bonded interactions which appear to follow the same trends as Ar–HF. As we have noted the vibrational frequency intervals do show a dependence upon the Ar–HF orientation, together with a dependence upon HF valence vibrational state, which may readily be surmised from the results shown in Fig. 5(a).

Table I lists all the observed spectroscopic constants for ArHF at $v=3$. The agreement between calculation based on Hutson's H6(4, 3, 2) potential,[11] whose parameters are ob-

tained from the levels $v_{HF}=0-2$, and observation is quite good. The theory predicted the band origins for the newly observed (3111) and (3101) bend-stretch combination states within 0.3 cm^{-1} without any re-optimization of the potential parameters. The excellent agreement between the present observations and the earlier predictions show the adequacy of Hutson's H6(4, 3, 2) potential for the ArHF states correlating asymptotically to HF $j=0$ and $j=1$. Since the present experiments test the predictions for $v_{HF}=3$ from the potential parametrized at lower valence vibrational levels of HF, we take this as a likely indication that at least as good of a fit should be obtained for the levels ($v101$) and ($v111$) for $v=0-2$ as found for $v=3$. As is seen from the change in rotational constants with van der Waals stretching excitation there is an appreciable increase in vdW bond length, R, upon its vibrational excitation. The good agreement between observation and prediction argues that Hutson's H6(4, 3, 2) is accurate for bound states correlating with $v=0-3$, $j=0-1$. However, as elaborated by Chang *et al.*,[11] a significant discrepancy of 1.7 cm^{-1} between experiment and calculation has been found in the (3210) HF $j=2$ bending state. In view of the excellent agreement for the lower bending states, it seems definite that the higher angular terms in the potential, particularly their HF valence state dependence, require further refinement. We hope to further examine this problem by probing the higher angular $\Delta(j_{HF}=2)$ bending/stretching combination states via the (0110) hot band excitation, transitions to which are forbidden directly from the (0000) ground state. Spectral characterization of these metastable states might allow us to explore the interesting parity-dependent rotational dissociation dynamics, as well as providing more information on the higher order angular terms necessary for the refinement of the Ar–HF H6(4, 3, 2) potential.

In the present work we have observed that upon van der Waals bond stretching excitation, there is a 20% increase in the energy splitting between HF ($j=1$) Σ and Π bending states for ArHF at $v=3$. Since the anisotropy of the interaction potential *decreases* with increasing internuclear separation R, as shown in Fig. 5, this observed increase in $\Sigma-\Pi$ splitting is at first sight surprising. The separation of the $j=1\Sigma$ and Π levels (310n) and (311n) may be thought of most simply in terms of the P_1 and P_2 terms of the interaction potential. For a large P_1 relative to P_2 in the attractive branch of the potential the Σ state will lie above the Π state. For ArHF, as has been known for 20 years, the P_2 term is dominant. It is seen from Fig. 5(b) that the anisotropy is reduced upon intermolecular radial vibrational excitation. Note that for all three of the exhibited states, the state with radial vibrational excitation is closer in form to the free rotor limit of the angular distribution ($\sin\theta,\cos^2\theta\sin\theta,\sin^3\theta$). Thus the increase in separation of the $j=1\Sigma$ and $\Pi(310n)$ and $(311n)$ levels containing radial vibrational excitation must be essentially due to the reduction of P_1 relative to P_2. This effect is amplified, since perturbatively P_2 appears in first order while P_1 has only a second order effect. The change in anisotropy splitting of the $j=1$ pair (310n) and (311n) with radial stretching excitation is well predicted by Hutson's H6(4,3,2)

potential as noted. This change is also well predicted by our *ab initio* calculation, as seen in Table III.

We gain further insight by examining the value of the Coriolis perturbation parameter q_l or β. The Hamiltonian for two molecular units coupled by a weak intermolecular potential has been discussed in detail by Brocks *et al.*[38] The rotational Hamiltonian of the ArHF complex can be expressed as:

$$\frac{1}{2\mu R^2}(\hat{\mathbf{J}}-\hat{\mathbf{j}})^2=\frac{1}{2\mu R^2}[\hat{\mathbf{J}}^2+\hat{\mathbf{j}}^2-\hat{J}_z^2-\hat{j}_z^2-(\hat{J}_+\hat{j}_++\hat{J}_-\hat{j}_-)].$$
(8)

where the equality $\hat{J}_z=\hat{j}_z$ for this system has been used. Terms involving $\hat{\mathbf{j}}$, the HF subunit angular momentum, are conventionally incorporated into the vibrational energy, while terms involving $\hat{\mathbf{J}}$ produce

$$\frac{1}{2\mu R^2}(\hat{\mathbf{J}}^2-\hat{J}_z^2)=B[J(J+1)-l^2].$$
(9)

The Coriolis contribution, $-(1/2\mu R^2)(\hat{J}_+\hat{j}_++\hat{J}_-\hat{j}_-)$, is

$$\langle J\Pi|-(1/2\mu R^2)(\hat{J}_+\hat{j}_++\hat{J}_-\hat{j}_-)|J\Sigma\rangle=\beta[J(J+1)]^{1/2},$$
(10)

where

$$\beta=B\langle\Pi|\hat{j}_+|\Sigma\rangle,$$
(11)

since as is seen in Table I the rotational constants of the Σ and Π states, (3101) and (3111), are essentially identical. The value of β for these two states is 0.156, or $\langle\Pi|\hat{j}_+|\Sigma\rangle=1.72$, relatively close to and somewhat greater than $\sqrt{2}$, which would be obtained in the asymptotic limit of $j=1$. It is noteworthy that Healey and Hutson *et al.* (Ref. 11) have deperturbed the somewhat more complex interactions of (3100) and (3110) and obtained $\beta=0.153$. Since the average of the rotational constants for (3100) and (3110) is 0.102 cm^{-1}, the value of $\langle\Pi|\hat{j}_+|\Sigma\rangle=1.50$ is closer to the asymptotic limit of $j=1$, a result at first somewhat surprising. The contribution of $j=0$ to (3100) is greater than to (3101) as is seen clearly in Fig. 6. It is interesting that estimates of the matrix elements of the Coriolis Hamiltonian are relatively close to the value in the asymptotic limit.

Finally, we briefly discuss the experimentally observed ArHF band intensities. The integrated band intensity ratio of (3001)←(0001), (3101)←(0001), and (3111)←(0001) is 5:2:1, the same as that of the corresponding (3000), (3100), and (3110) bands originating from the (0000) ground state.[10] From the lack of observation of features of the (3001)←(0000) transition, we conclude that the intensity of this transition is at least 3000 times weaker than that of the (3000)←(0000) transition. By contrast, the corresponding (1001)←(0000) band has been observed by Nesbitt *et al.*[7] with an intensity 5×10^{-3} times that of (1000)←(0000). However, as pointed out by Nesbitt *et al.*, the (1001)←(0000) band intensity is calculated to be 5.5×10^{-4} times that of the (1000)←(0000) band based upon Fraser and Pine's Ar+HF($v=0$) 1D radial potential,[4] which is still an order of magnitude weaker than the experimental observation. Note that the energy spacing between the (1100) and (1001) states is 16.000 cm^{-1} while it is 26.710 cm^{-1} between the (3100) and (3001) states. Thus, it is highly likely

J. Chem. Phys., Vol. 112, No. 16, 22 April 2000

Ar–HF at $v_{HF}=3$ 7031

that the strong bend-stretch anharmonic coupling between those two states in ArHF at $v=1$ is responsible for the bright transition (intensity borrowing) of $(1001) \leftarrow (0000)$, and that this coupling is diminished dramatically at $v=3$ as the (3100) state is further separated from the (3001) state. This is a further manifestation of the increasing anisotropy of the potential as a function of the increasing HF bond length, or equivalently the HF valence vibration.

VI. SUMMARY

Three new bands of ArHF [(3001), (3101), and (3111)] have been observed via (0001) hot band excitation using intracavity laser induced fluorescence. In conjunction with the previously observed five ArHF ($v=3$) bands, a total of eight ArHF states at $v=3$ (and overall 33 vibrational states to date for $v_{HF}=0$ to 3) provide more information for the Ar–HF ($v=3$) interaction potential. We have solved the puzzle of the ArHF ($v=3$) hydrogen bond or van der Waals stretch frequency ($=46.894$ cm^{-1}) by the observation of the $(3001) \leftarrow (0001)$ hot band transition. The van der Waals stretching frequencies have been found to linearly increase as the HF valence bond is elongated from $v_{HF}=0$ to 3. The energy splitting between the Σ and Π bending states increases 20% upon van der Waals stretch excitation indicating that the radially averaged potential anisotropy is strongly dependent on the intermolecular bond length. Predictions from the H6(4,3,2) potential show excellent agreement with the experimental results correlated to HF $j=1$ and $j=0$ bend/stretch states. The only significant discrepancy (1.7 cm^{-1}) begins to show in the (3210) bending state (correlated to HF $j=2$) and this strongly suggests that refinement of the higher order angular terms in the H6(4,3,2) potential is necessary. Refinement of the Ar–HF pair potential appears to be necessary to fully understand the photodissociation dynamics of ArHF occurring at highly vibrationally excited states as well as the interaction potential and the nature of the three-body forces in Ar$_2$HF.

A CCSD(T) ab initio calculation provides insight into the explicit r_{HF} dependence of the Ar–HF interaction potential. It is seen that in the linear Ar–HF configuration the HF bond can stretch to 1.5 Å before argon–hydrogen repulsion is apparent, while, as expected, this repulsion is not seen for the T shaped and anti-linear configurations. Preliminary bound state calculations indicate that the effects of this repulsion should become evident through a reduction in the rotational constant for $(v000)$ at $v_{HF}=5$.

ACKNOWLEDGMENTS

[1] S. J. Harrris, S. E. Novick, and W. Klemperer, J. Chem. Phys. **60**, 3208 (1974); T. A. Dixon, C. H. Joyner, F. A. Baiocchi, and W. Klemperer, ibid. **74**, 6539 (1981).

[2] M. R. Keenan, L. W. Buxton, E. J. Campbell, A. C. Legon, and W. H. Flygare, J. Chem. Phys. **74**, 2133 (1981); P. A. Stockman and G. A. Blake, ibid. **98**, 4307 (1993).

[3] M. A. Dvorak, S. W. Reeve, W. A. Burns, A. Grushow, and K. R. Leopold, Chem. Phys. Lett. **185**, 399 (1991).

[4] G. T. Fraser and A. S. Pine, J. Chem. Phys. **85**, 2502 (1986).

[5] C. M. Lovejoy, M. D. Schuder, and D. J. Nesbitt, Chem. Phys. Lett. **127**, 374 (1986); J. Chem. Phys. **85**, 4890 (1986).

[6] Z. S. Huang, K. W. Jucks, and R. E. Miller, J. Chem. Phys. **85**, 6905 (1986).

[7] C. M. Lovejoy and D. J. Nesbitt, J. Chem. Phys. **91**, 2790 (1989).

[8] A. McIlroy and D. J. Nesbitt, Chem. Phys. Lett. **187**, 215 (1991); J. T. Farrell, Jr., O. Sneh, A. McIlroy, A. E. Knight, and D. J. Nesbitt, J. Chem. Phys. **97**, 7967 (1992).

[9] C. M. Lovejoy, J. M. Hutson, and D. J. Nesbitt, J. Chem. Phys. **97**, 8009 (1992).

[10] H.-C. Chang and W. Klemperer, J. Chem. Phys. **98**, 2497 (1993).

[11] H.-C. Chang, F.-M. Tao, W. Klemperer, C. H. Healey, and J. M. Hutson, J. Chem. Phys. **99**, 9337 (1993).

[12] The ArHF state is designated by the label $(vbKn)$, where v denotes the HF valence stretching quantum number, b is the bending quantum (which correlates with the diatom rotational quantum number j in the free-rotor limit), K is the projection of rotational angular momentum on the molecular axis, and n is the van der Waals stretching quantum number (see Ref. 17).

[13] C.-C. Chuang, S. N. Tsang, W. Klemperer, and H.-C. Chang, J. Chem. Phys. **109**, 8836 (1998).

[14] P. A. Block and R. E. Miller, Chem. Phys. Lett. **226**, 317 (1994).

[15] F.-M. Tao and W. Klemperer, J. Chem. Phys. **101**, 1129 (1994).

[16] T. van Mourik and T. H. Dunning, Jr., J. Chem. Phys. **107**, 2451 (1997).

[17] J. M. Hutson, J. Chem. Phys. **96**, 6752 (1992).

[18] R. A. Aziz, in Inert Gases, edited by M. L. Klein (Springer, Berlin, 1989), p. 5.

[19] A. Ernesti and J. M. Hutson, Phys. Rev. A **51**, 239 (1995).

[20] C.-C. Chuang, S. N. Tsang, W. Klemperer, and H.-C. Chang, J. Chem. Phys. **107**, 7041 (1997).

[21] C.-C. Chuang, S. N. Tsang, W. Klemperer, and H.-C. Chang, J. Phys. Chem. A **101**, 6702 (1997).

[22] The sign of the l-doubling constant follows $\Delta E_{ef}=E_e-E_f$ [K. P. Huber and G. Herzberg, Molecular Spectra and Molecular Structure, IV (Van Nostrand-Reinhold, New York, 1979)].

[23] K. J. Higgins and W. Klemperer (in preparation).

[24] T. H. Dunning, Jr., J. Chem. Phys. **90**, 1007 (1989).

[25] R. A. Kendall, T. H. Dunning, Jr., and R. J. Harrison, J. Chem. Phys. **96**, 6796 (1992).

[26] D. E. Woon and T. H. Dunning, Jr., J. Chem. Phys. **98**, 1358 (1993).

[27] F.-M. Tao and Y.-K. Pan, J. Chem. Phys. **97**, 4989 (1992).

[28] J. A. Coxon and P. G. Hajigeorgiou, J. Mol. Spectrosc. **142**, 254 (1990); W. T. Zemke, W. C. Stwalley, A. Coxon, and P. G. Hajigeorgiou, Chem. Phys. Lett. **177**, 412 (1991).

[29] W. T. Zemke, W. C. Stwalley, S. R. Langhoff, G. L. Valderrama, and M. J. Berry, J. Chem. Phys. **95**, 7846 (1991).

[30] R. D. Hasse, M. W. Severson, M. M. Szczesniak, G. Chalasinski, P. Cieplak, R. A. Kendall, S. M. Cybulski, J. Mol. Struct. **436–437**, 387 (1997); K. W. Chan, T. D. Power, J. Jai-nhuknan, and S. M. Cybulski, J. Chem. Phys. **110**, 860 (1999); S. M. Cybulski, J. Couvillion, J. Klos, and G. Chalasinski, ibid. **110**, 1416 (1999).

[31] S. F. Boys and F. Bernardi, Mol. Phys. **19**, 553 (1970).

[32] MOLPRO is a package of ab initio programs written by H.-J. Werner and P. J. Knowles, with contributions from J. Almlöf, R. D. Amos, A. Berning, D. L. Cooper, M. J. O. Deegan, A. J. Dobbyn, F. Eckert, S. T. Elbert, C. Hampel, R. Lindh, A. W. Lloyd, W. Meyer, A. Nicklass, K. Peterson, R. Pitzer, A. J. Stone, P. R. Taylor, M. E. Mura, P. Pulay, M. Schütz, H. Stoll, and T. Thorsteinsson.

[33] Modified from W. H. Press, B. P. Flannery, S. A. Teukolsky, and W. T. Vetterling, Numerical Recipes: The Art of Scientific Computing (Cambridge University Press, New York, 1986), Chap. 3.

[34] V. F. Lotrich, H. L. Williams, K. Szalewicz, B. Jeziorski, R. Moszynski, P. E. S. Wormer, and A. van der Avoird, J. Chem. Phys. **103**, 6076 (1995).

[35] R. C. Cohen and R. J. Saykally, J. Chem. Phys. **95**, 7891 (1990); **98**, 6007 (1993).

[36] J. M. Hutson, BOUND computer code, version 5 1993, distributed by Collaborative Computational Project No. 6 of the Science and Engineering Research Council (UK).

[37] C. H. Townes and A. L. Schawlow, Microwave Spectroscopy (McGraw-Hill, New York, 1955).

[38] G. Brocks, A. van der Avoird, B. T. Sutcliffe, and J. Tennyson, Mol. Phys. **50**, 1025 (1983). Note that the shift operators are defined as $\hat{J}_\pm = \hat{J}_x \mp i\hat{J}_y$ and $\hat{j}_\pm = \hat{j}_x \pm i\hat{j}_y$ for partially body fixed axis systems.